Cellulose (2015) 22:1943–1953
DOI 10.1007/s10570-015-0606-2

ORIGINAL PAPER

Effect of xylan content on mechanical properties in regenerated cellulose/xylan blend films from ionic liquid

Johan Sundberg · Guillermo Toriz · Paul Gatenholm

Received: 26 August 2014 / Accepted: 14 March 2015 / Published online: 25 March 2015
© Springer Science+Business Media Dordrecht 2015

Abstract We report of cellulose and arabinoglucuronoxylan (AGX) blend films made from wood polymers extracted from one and the same tree. Blends were prepared by dissolution of wood polymers in 1-ethyl-3-methylimidazolium acetate (EmimAc). Films were produced by casting EmimAc solution followed by coagulation in ethanol. The films were optically transparent, fully amorphous as shown by wide angle X-ray scattering, and free from EmimAc residues as shown by Fourier transform infrared spectroscopy. Mechanical properties were analyzed as a function of water content. The plasticizing effect of water on the films was evidenced by both tensile and dynamical mechanical analysis measurements with humidity scans. Equilibrium moisture content (w/w) was measured at different relative humidities and the proportional water uptake was clearly related to the mechanical properties. We found good mechanical properties independent of the polysaccharide composition and an increased Young's modulus at low humidities with a maximum at approximately 20 % AGX content. The strengthening effect was removed after leaching the AGX from the films. This study shows potential applications of biopolymer extracted from trees as future packaging.

Keywords Wood biopolymers films · Ionic liquid · Mechanical properties · Arabinoglucuronoxylan

Introduction

The secondary cell wall in plants has a highly organized hierarchical structure with exceptional properties (Albersheim et al. 2010). Cellulose and hemicelluloses are the two main components in the cell wall and they constitute a renewable and biodegradable resource with great potential (Ragauskas et al. 2006; Zhu et al. 2006). Hemicelluloses are complex polysaccharides composed of a different number of sugar units and their derivatives that have a relatively low degree of polymerization (~70–200 sugar units) (Heredia et al. 1995; Ragauskas et al.

Electronic supplementary material The online version of this article (doi:10.1007/s10570-015-0606-2) contains supplementary material, which is available to authorized users.

J. Sundberg · G. Toriz · P. Gatenholm
Wallenberg Wood Science Center, Göteborg, Sweden

J. Sundberg · P. Gatenholm (✉)
Biopolymer Technology, Department of Chemistry and Chemical Engineering, Chalmers University of Technology, 412 96 Göteborg, Sweden
e-mail: paul.gatenholm@chalmers.se

G. Toriz
Department of Wood, Cellulose and Paper Research, University of Guadalajara, Guadalajara, Jalisco, Mexico

2006). Hemicelluloses represent a vast natural resource as they account for the majority of plant biomass after cellulose and lignin (Lerouxel et al. 2006; Reiter 2002). Hemicelluloses are often divided into four main classes, e.g. xyloglucans, glucomannans, xylans and mixed linkage glucans. Xylans are the most abundant hemicelluloses (Fengel and Wegener 1983), and depending on their native chemical structure, molecular weight and branched character they may be soluble in water. Strong interactions within cellulose chains (Klemm et al. 2005) and with the hemicellulose matrix provides for the great mechanical performance of the secondary cell wall (Albersheim et al. 2010), that could be utilized for high performance materials.

The macromolecular structure of cellulose makes it insoluble in water (Hauru et al. 2012; Lindman et al. 2010; Medronho and Lindman 2014; Medronho et al. 2012), which complicates industrial processing. Ionic liquids (IL) can be used to dissolve cellulose and hemicelluloses (Kilpeläinen et al. 2007; Swatloski et al. 2002) and they do not cause the polymer chains to degrade at moderate temperatures (Mäki-Arvela et al. 2010). ILs are composed of molten salts that are liquid at ambient temperatures, have a low vapor pressure and are chemically stable (El Seoud et al. 2007; Rogers and Seddon 2003; Torimoto et al. 2009; Zhu et al. 2006). The dissolution potential of cellulose and hemicellulose in the ionic liquid 1-Ethyl-3-methylimidazolium acetate (EmimAc) is not decreased to the same extent by the presence of water in the ionic liquid (Hauru et al. 2012) as other ILs are (Swatloski et al. 2002; Troshenkowa and Wawro 2010).

Dissolution and regeneration of lignocellulosic materials from ionic liquids have previously been described in the literature (Kosan et al. 2008; Pinkert et al. 2009; Simmons et al. 2011; Sundberg et al. 2013; Turner et al. 2004; Zhao et al. 2009). The crystallinity of regenerated materials depends upon the dissolution time and the regeneration conditions. Both partially crystalline materials (Cao et al. 2010; Zhang et al. 2005; Östlund et al. 2013) as well as amorphous materials (Kilpeläinen et al. 2007; Sundberg et al. 2013; Wu et al. 2009) have been reported. The non-solvent used for regeneration also affects the properties of the regenerated materials (Fink et al. 2001; Isobe et al. 2011; Östlund et al. 2013). The tunable crystallinity provides a tool to customize the material properties for specific applications.

Water plasticizes cellulose (Nakamura et al. 1983; Salmen and Back 1977; Sundberg et al. 2013) by absorption to the amorphous parts of the polymer matrix (Howsmon 1949; Zografi et al. 1984) and therefore, the amount of molecularly bound water is inversely proportional to the degree of crystallinity of the cellulose (Nakamura et al. 1981). In contrast to cellulose most of hemicelluloses are water soluble, a fact that is however affected by their chemical structure (Bosmans et al. 2014). As a consequence at RHs above 75 % AGX films flow freely with rapidly decreasing storage modulus (Escalante et al. 2012). Xylan has been shown to strengthen cellulose/xylan composites (Dammström and Gatenholm 2008; Köhnke et al. 2008; Sun et al. 2014) with a maximum in the Young's modulus at approximately 30 % xylan content (Dammström and Gatenholm 2008).

Hemicelluloses, specifically xylan, have good mechanical properties (Gröndahl et al. 2004; Höije et al. 2008; Šimkovic et al. 2014). That can be explained by their chemical structure and molecular weight (Mw). For instance Šimkovic et al. (2014) reported xylan (Mw 45,000 Da; 17 % 4-O-MeGlcA content, 83 % xylose) films with high Young's modulus (7 GPa) and tensile strength (around 100 MPa) with 4 % elongation to break. Escalante et al. (2012) reported on spruce AGX (Mw 12,700 Da, 10 % 4-O-MeGlcA content, 80 % xylose, 7 % arabinose, 3 % other sugars) films with Young's modulus around 2.7 GPa, tensile strength 55 MPa and 2.7 % strain to break and very low oxygen permeability.

A better understanding of the molecular and supramolecular interactions between cellulose and xylan could lead to novel materials with tailored properties. It could also contribute to an increased use of this abundant but not fully utilized biopolymer.

In this study we analyze the structure, crystallinity and mechanical properties of cellulose/AGX blend films as a function of moisture. The two biopolymers used were isolated from the cell wall of a single Norwegian spruce, dissolved in, and precipitated from EmimAc with ethanol.

Materials and methods

Cellulose isolation from spruce wood

Spruce cellulose was isolated by chlorite delignification according to the Wise and Timell methods

(Timell 1961; Wise et al. 1946). Briefly, 150 g of wood meal (Norway Spruce) was delignified with sodium chlorite at 70–80 °C, in a three-necked round flask in the following manner: To a 1:25 wood meal to liquor ratio (adjusted with water) glacial CH_3COOH and $NaClO_2$ (15 mL: 45 g respectively) were added every 12 h four times. The obtained holocellulose (about 100 g) was then treated with 24 wt% KOH in a ratio 1:7 w:v for 24 h at room temperature in order to extract 4-O-methyl-glucuronoarabinoxylan and galactoglucomannans. The non-soluble material was treated with a mixture of sodium hydroxide (17.5 wt%) and boric acid (4 wt%) at room temperature for 24 h to extract glucomannans. The obtained cellulose was washed with diluted acetic acid until neutral pH and air dried on the lab bench.

Arabinoglucuronoxylan extraction from spruce wood

Hemicelluloses were precipitated from the 24 wt% KOH extract from holocellulose (vide supra) with acidic ethanol (hemicellulose solution: ethanol 96 %: glacial CH_3COOH in a ratio 1:4:0.4 v:v:v respectively), filtrated, dried and again dissolved in 10 wt% KOH (1:10 w:v) at room temperature for about 30 min. The latter hemicellulose solution was treated with a saturated solution of $Ba(OH)_2$ (1:20 w:v) to precipitate the galactoglucomannans, which afterwards were separated by centrifugation. The supernatant containing AGX was poured into a solution of acidic ethanol as described above in order to obtain AGX with a yield of approximately 10 g (7 wt% from the original wood).

Arabinoglucuronoxylan was further bleached with hydrogen peroxide as it follows: 1:20 hemicellulose to water ratio was set and 1.2 wt% diethylene triamine pentaacetic acid (DTPA) was added and left overnight in order to chelate any metal that could inactivate the peroxide. Sodium silicate and hydrogen peroxide (2.25 and 30 wt% respectively, referred to the xylan content) were added, the temperature was raised to 50 °C and the pH adjusted with NaOH 1 N to 10.5–11.0. The bleaching reaction time was 4 h after which, arabinoglucuronoxylan was precipitated in four volumes of acidic ethanol as mentioned before, filtered in Whatman filter paper and dried in vacuum.

The molecular weight of the AGX was analyzed using a Waters 2690 aqueous system (Waters Corporation, USA) consisting of HPSEC-MALS-RI-UV as described in detailed by Escalante et al. (2012) and was determined to be Mw 12,700 Da. The sugar composition of the AGX was analyzed using HPAEC-PAD (Dionex) and was determined to be 10 % 4-O-MeGlcA, 80 % xylose, 7 % arabinose, 3 % other sugars.

Film preparation

Five different films were prepared by varying the amount of arabinoglucuronoxylan (AGX) [0 % AGX, 5 % AGX, 10 % AGX, 20 % AGX and 33 % AGX (w/w) of the total dry weight]. A total dry weight of 0.5 g were solubilized in 12.5 g of EmimAc (BASF, Sigma-Aldrich) at 80 °C for 96 h after which the solution was clear and homogeneous. The solution was poured onto glass and spread to a thickness of 0.5 mm using a glass slide. The thin spread liquid solution was placed in an oven at 80 °C for a few minutes to smoothen the surface. The solution was then sprayed with 99.9 % ethanol (Scharlau, Fisher Scientific) using an atomizing nozzle (LEE Company). Once the surface of the solution coagulated, the glass was submerged in an ethanol bath to allow for full gelation. The formed gel was then washed by repeated exchange of ethanol to remove all the EmimAc. The pure gels were dried at room temperature on sheets of Teflon in sealed containers over a saturated salt solution of $(MgNO_3)_2{\cdot}6H_2O$ (Acros, Sigma-Aldrich) providing a relative humidity (RH) of 54 %. The dried films were 25 ± 9 μm thick.

Carbohydrate analysis (Dionex)

The carbohydrate composition was analyzed in triplicates with high performance anion exchange chromatography with pulsed amperometric detection (HPAEC-PAD), using a Dionex ICS-3000 system equipped with a CarboPac PA1 (4 × 250 mm) analytical column. Prior to analysis the samples were hydrolyzed according to Theander and Westerlund (Theander and Westerlund 1986).

Scanning electron microscopy (SEM)

Samples for SEM analysis were kept at 0 % RH for 7 days until analysis. Cross sections were prepared by quenching the films in liquid N_2 followed by snapping or carefully ripping them into pieces. Cutting tools

were avoided to ensure the preservation of the internal structure of the films. Several cross sections were analyzed for each film. The samples were mounted onto stubs and sputter coated for 60 s with gold (Edwards Sputter Coater S150B). The samples were analyzed using a Leo Ultra 55 FEG SEM.

X-ray diffraction analysis (XRD)

The crystallinity of the regenerated films was analyzed using wide angle x-ray scattering (WAXS). Samples were mounted on glass slides and analyzed with Phillips X'Pert materials research diffractometer (MRD). Radiation was generated with an X-ray tube with Cu anode (Kα radiation, $\lambda = 1.54184$ Å) at 45 kV and 40 mA. The 2θ range was 10°–30°, and the resolution was 0.1° with 6 s averaging time per step.

Control powder samples of AGX and Spruce cellulose were analyzed with a Siemens D5000 in Bragg–Brentano set-up using Cu-characteristic radiation (1.54056 Å) and a secondary monochromator. The 2θ range was 10–30°, and the resolution was 0.05°.

Fourier transform infrared spectroscopy (FTIR)

Samples to be analyzed were stored at 0 % relative humidity. Thin samples of the films were analyzed using beam condenser mode. The spectrum from 4000 to 400 cm^{-1} was recorded for each sample with a resolution of 4 cm^{-1}. The spectrum for EmimAc was acquired by placing a small droplet of EmimAc in between two tablets of KBr. All samples were analyzed using a Perkin Elmer 2000 FTIR. The EmimAc data was normalized against a pellet of pure KBr.

Tensile testing

The tensile tests were conducted in a DMA Q800 (TA Instruments) with an attached RH control unit to allow for controlled relative humidity during the tests. Samples were cut from the films using parallel razor blades with an inter distance of 5.73 mm. The film thickness (average of three measurements) was measured using a Micrometer (Mitutoyo). The samples were mounted in the testing chamber with an approximate distance between the clamps of 14 mm. The samples were then allowed to equilibrate to the desired humidity before testing commenced. The temperature was set to 25 °C. A preload of 0.01 N was used and the stress was ramped with 0.25 N/min. Due to the complexity for setting up this test only three replicates were tested for each film at each humidity.

Dynamical mechanical analysis (DMA)

Dynamical mechanical analysis (DMA) was used to measure the storage modulus (G') of the regenerated films. The measurements were conducted using a DMA Q800 (TA Instruments) connected to a humidity controller. Samples for analysis were cut from the films using parallel razor blades with an inter distance of 5.73 mm. The film thickness (average of three measurements) was measured using a Micrometer (Mitutoyo). The samples were mounted in the testing chamber with an approximate distance between the clamps of 15 mm. The samples were loaded at 1 Hz frequency, 125 % force track, 0.1 N preload force and an amplitude of 10 μm. The temperature was fixed at 25 °C and the humidity was ramped with 1 % RH per 10 min starting at 10 % RH running up to 90 % RH. The data was normalized.

Water vapor sorption

Film samples (0 % AGX; 20 % AGX and 33 % AGX) were conditioned in closed vessels containing saturated salt solutions. The salts used were lithium chloride (LiCl; Sigma-Aldrich), magnesium chloride hexahydrate ($MgCl_2 \cdot 6H_2O$; Merck, Sigma-Aldrich), magnesium nitrate hexahydrate ($Mg(NO_3)_2) \cdot 6H_2O$; Acros, Sigma-Aldrich), sodium chloride (NaCl; Merck, Sigma-Aldrich) and potassium sulphate (K_2SO_4; Sigma-Aldrich) giving relative humidities (RH) of 11, 33, 54, 75 and 97 % respectively. For 100 % RH the samples were conditioned over deionized water. The samples were dried at 105 °C for 1 h and then stored in a desiccator at 0 % RH. The samples were weighed and then conditioned at the lowest humidity for 24 h. The weight was recorded and the samples were then moved to the next increased sequential humidity and left for 24 h before the next measurement.

Arabinoglucuroxylan leaching

Films (0 % AGX, 20 % AGX and 33 % AGX) were placed in 5 wt% KOH solution at 40 °C and stirred at

150 rpm. The KOH solution was exchanged three times with approximately 12 h in between changes. The films were then placed in deionized water at 40 °C and stirred at 150 rpm. The water was exchanged twice with approximately 12 h in between changes. The films were dried at room temperature on sheets of Teflon in sealed containers over a saturated salt solution of $(MgNO_3)_2{\cdot}6H_2O$ (Acros, Sigma-Aldrich) providing a RH of 54 %.

Statistical analysis

Statistical analyses were performed using Microsoft Excel 2010 Software (Microsoft). The sample size from the tensile tests was n = 3 per data point. Each data point is reported as the mean ± standard deviation. One-way ANOVA utilizing Bonferroni-Holm posthoc analysis was used to compare all pairs of means. p values of $p < 0.05$ were considered to be statistical significant.

Results and discussion

Regeneration and film morphology

The regeneration process resulted in clear optically transparent thin films with a smooth surface. Regarding optical transparency, little to no difference was observed for films of different composition. These observations suggest that both the cellulose and the arabinoglucuronoxylan were solubilized in the EmimAc and that the components were fully miscible. The macromorphology of the 5 % w/w arabinoglucuronoxylan film can be seen in Fig. 1. FTIR spectra of the regenerated films lacked the characteristic peaks of the pure EmimAc (1572 and 1404 cm^{-1}) (Supplement Fig S1) and thus confirmed the removal of EmimAc from the regenerated materials. Carbohydrate composition analysis revealed that the initial blend ratios were not maintained after regeneration (Table 1). Residues were seen on the glass used to cast the films. It was also noted that the adherence of the films to the glass increased with increasing arabinoglucuronoxylan content. The regeneration process consequently resulted in arabinoglucuronoxylan losses.

X-ray diffraction analysis showed that the non-regenerated cellulose was semi-crystalline and that the non-regenerated arabinoglucuronoxylan was amorphous. Regenerated films were all amorphous and there was little to no variation in between films with different composition (Fig. 2). Consequently the arabinoglucuronoxylan content did not affect the crystallinity of the regenerated films. Low film thickness in combination with ethanol (Östlund et al. 2013) as a non-solvent also ensured a rapid regeneration process, which subsequently resulted in amorphous films.

Fig. 1 Regeneration of cellulose/AGX blends from EmimAc results in clear and optically transparent films. The film depicted is a 5 % AGX film

Figure 3 shows SEM images of surface and cross section of 0 % AGX, 20 % AGX and 33 % AGX films. As seen the surface of the films is smooth while the cross section shows a porous laminar structure with little to no variation between the films with different composition. Results of SEM analysis support the proposed gelling mechanics of a spinodal decomposition resulting in a film with internal porosity on a nano level (Laity et al. 2002; Sundberg et al. 2013). The observed similarity between the films of different composition could potentially be explained by a regeneration process where a network of cellulose forms independently of the arabinoglucuronoxylan content. The arabinoglucuronoxylan can then adsorb on the cellulose network as well as agglomerate in the empty voids in the cellulose network. Froschauer et al. (2013) showed that there is a difference in solubility between cellulose and xylan in an EmimAc/ethanol solvent system, with cellulose displaying a lower solubility than xylan with an increasing ethanol concentration. During the regeneration process where ethanol is added to the EmimAc solution this would likely result in a phase separation further explaining the morphology of the films.

Table 1 Carbohydrate analysis of regenerated films. The results are reported as the mean value (n = 3) ± the standard deviation

Sample	Detected glucose (mg/L)	Detected xylose (mg/L)	AGX fraction (%)[a]
0 % AGX	148.90 ± 3.82	0.00	0
5 % AGX	139.76 ± 3.58	3.09 ± 0.18	3.05
10 % AGX	136.82 ± 3.46	5.99 ± 0.21	5.89
20 % AGX	127.72 ± 3.34	13.33 ± 0.44	12.94
33 % AGX	105.43 ± 2.89	21.42 ± 0.70	22.44

[a] The AGX fraction was calculated from the molar fractions proposed by Escalante et al. (2012)

Water sorption isotherms

Equilibrium water content of the films (0 % AGX, 20 % AGX and 33 % AGX) was analyzed at different RH. The films were conditioned over saturated salt solutions in closed containers. The absorption curve of the films was recorded and the results can be seen in Fig. 4. Water uptake of the samples was approximately linear until a RH of 75 %. For RH above 75 % the recorded water uptake was considerably higher. This change in the water uptake rate could be due to a change in the conformation of absorbed water within the material from bound to free water (Froix and Nelson 1975; Sundberg et al. 2013). The increase could also be affected by increased biopolymer chain mobility facilitated by water plasticizing effect.

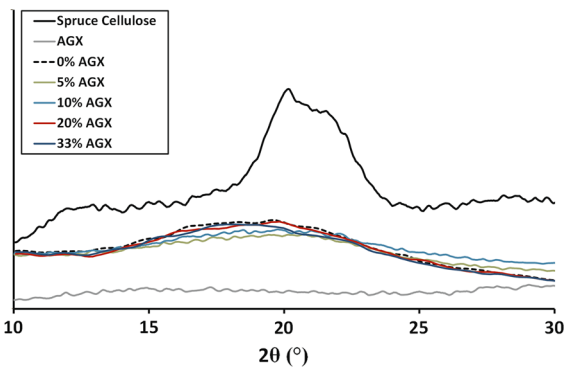

Fig. 2 Wide angle X-ray diffraction (WAXS) spectra of spruce cellulose, AGX and films regenerated from dissolved cellulose (0 % AGX) and cellulose/AGX blends (5 % AGX, 10 % AGX, 20 % AGX and 33 % AGX)

Mechanical properties

Dynamical mechanical analysis (DMA)

In Fig. 5 the results of the DMA analysis are shown. The change in the storage modulus as a function of the RH is similar between films of different composition with some differences in the absolute values at 10 %

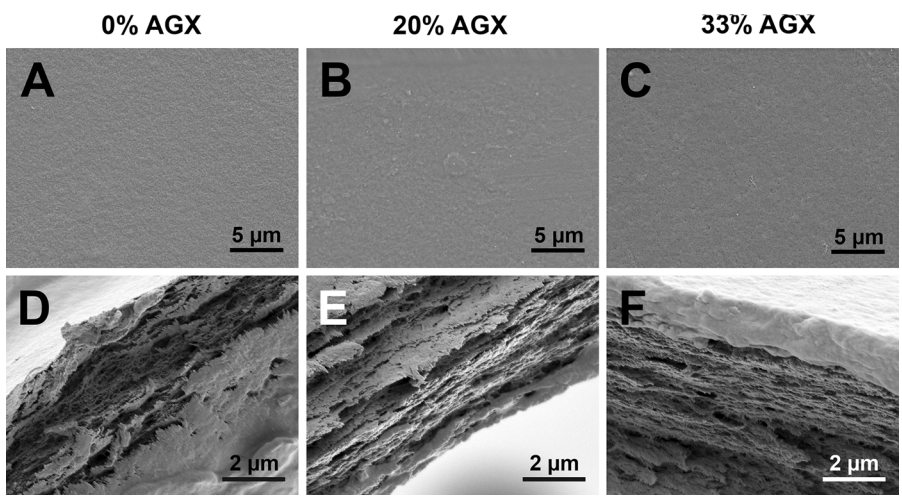

Fig. 3 Scanning electron micrographs of regenerated cellulose films (0 % AGX) (**a** and **d**) and cellulose/AGX blend films (**b** and **e**; 20 % AGX, **c** and **f**; 33 % AGX) top surface at ×10,000 magnification (**a**–**c**) and cross section at ×30,000 magnification (**d**–**f**)

RH (0 % AGX, 6870 MPa; 5 % AGX, 7883 MPa; 10 % AGX, 5909 MPa; 20 % AGX, 7644 MPa; 33 % AGX, 8578 MPa). All the different films were plasticized by moisture increase and starting at approximately 70 % RH the storage modulus decreased rapidly. The accelerated plasticization of the films could likely be attributed to a change in the conformation of absorbed water within the material (Froix and Nelson 1975; Sundberg et al. 2013), from molecularly bound to free, reaching a critical point at approximately 70 % RH. This corresponds well to the results from the water sorption isotherm analysis where the water uptake increases rapidly at approximately the same moisture content. The similarity of the plasticizing properties of the films supports the proposed regeneration kinetics with a cellulose network forming independently of the AGX content. The measured storage modulus is presumably only attributed to the cellulose component and not affected by the AGX content.

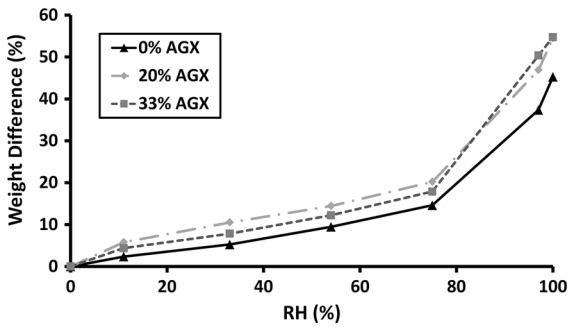

Fig. 4 The weight percent water as a function of the relative humidity for regenerated spruce cellulose (0 % AGX) and cellulose/AGX blends (20 % AGX and 33 % AGX)

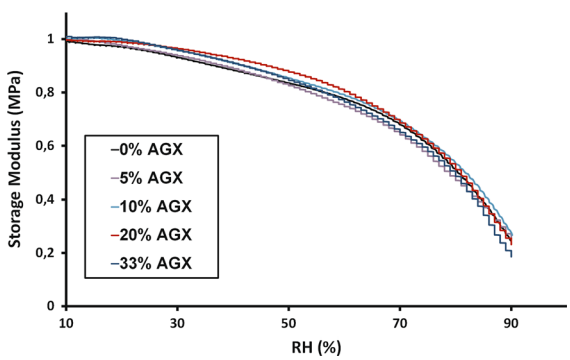

Fig. 5 The storage modulus (G′) as a function of the relative humidity for regenerated films of cellulose (0 % AGX) and cellulose/AGX blends (5 % AGX, 10 % AGX, 20 % AGX and 33 % AGX)

Tensile properties

Tensile tests were conducted in a DMA Q800 (TA Instruments) with an attached RH control unit to allow for controlled relative humidity. In Fig. 6 the stress strain behavior of each film composition is plotted for different RH. As it can be seen, films with different composition display similar tensile strength and deformation at all tested relative humidities. There was some variation in the maximum stress and toughness for the different film compositions, especially for the 33 % AGX samples, which partly could be due to the difficulty of exactly replicating the production process. The trend in water/cellulose interaction is clear with a decrease in stiffness and an increase in the strain at break with increasing relative humidity. The results of the blended films correspond well to the previously reported results of cellulose films with low to medium DP (Sundberg et al. 2013). The similarity of the different samples further adds to the proposed regeneration kinetics with a cellulose network forming independent of the arabinoglucuronoxylan content.

In Fig. 7 Young's moduli are plotted for the different films. The stiffness of the films decreases with an increasing RH. At 30 % RH the stiffness of the films containing AGX is higher than the pure cellulose films with the 20 % AGX films being the stiffest. Köhnke et al. (Köhnke et al. 2008) showed that the adsorption of (glucurono)arabinoxylan (GAX) to cellulose fibers improved the mechanical properties of material prepared from the modified fibers compared to unmodified cellulose fibers. Dammström and Gatenholm (2008) reported that addition of xylan in bacterial nanocellulose/xylan nanocomposites increased the Young's modulus with a maximum at 33 % xylan (w/w). Sun et al. (2014) showed that the tensile strength of cellulose nanowhiskers (CNW) films increased when Birch wood xylan was adsorbed onto the CNWs prior to casting. The authors attribute the increase in mechanical properties to the formation of a rigid hydrogen bonded network resulting from the strong and irreversible interaction between the CNW and xylan. At humidities below a critical plasticization level the addition of arabinoglucuronoxylan increases the tensile strength of the regenerated films. We

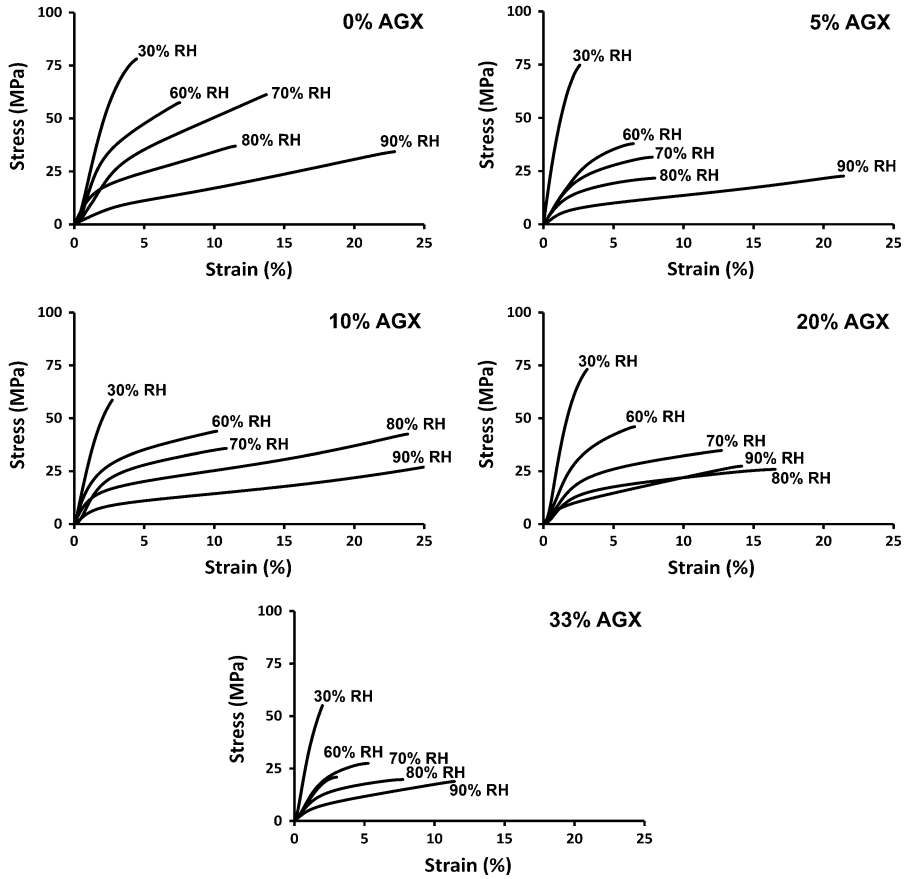

Fig. 6 Representative stress/strain plots of regenerated cellulose films (0 % AGX) and cellulose/AGX blend films (5 % AGX, 10 % AGX, 20 % AGX and 33 % AGX) at different relative humidities

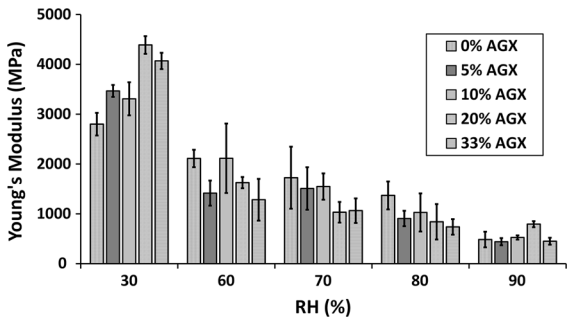

Fig. 7 Young's modulus of the regenerated cellulose (0 % AGX) and cellulose/AGX blend films (5 % AGX, 10 % AGX, 20 % AGX and 33 % AGX) at different relative humidities. Each bar represents three replicates ± the standard deviation. Statistical significant differences ($p \leq 0.05$) were seen between samples at 30 % RH (Fig. 8) and 90 % RH (20 % AGX different ($p \leq 0.05$) to 5 % AGX, 10 % AGX and 33 % AGX). All films were statistical significant different ($p \leq 0.05$) at 30 % RH compared to higher RH (apart from 0 % AGX 30 % RH compared to 60 % RH, 70 % RH; and 10 % AGX at 30 % RH compared to 60 % RH). Few differences in between samples at higher humidities were seen

hypothesize that this effect is due to increased adhesion in the regenerated cellulose with the arabinoglucuronoxylan acting as a binding matrix and that the effect is lost at higher humidities due to the strong plasticization of xylan by water. However, further investigation is needed to fully understand the mechanisms governing this effect. The xylan molecular structure also potentially affects the interactions with cellulose and subsequently the mechanical performance (Höije et al. 2008; Šimkovic et al. 2014).

Leaching of arabinoglucuronoxylan was successful and resulted in an almost complete removal of AGX from the films (Table 2). The strengthening effect of the arabinoglucuronoxylan was removed upon removal of the AGX from the films (Fig. 8). A correction for the change in density after leaching for the 20 % AGX films and 33 % AGX films does not fully explain the difference in modulus between these samples and the 0 % AGX films. The leaching results

Table 2 Carbohydrate analysis of regenerated films after leaching of AGX

Sample	Detected glucose (mg/L)	Detected xylose (mg/L)	AGX fraction (%)[a]
0 % AGX—after leaching	155.78 ± 4.79	0.00	0.00
20 % AGX—after leaching	141.03 ± 4.27	0.00	0.00
33 % AGX—after leaching	155.62 ± 4.21	0.03 ± 0.02	0.03

The results are reported as the mean value (n = 3) ± the standard deviation

[a] The AGX fraction was calculated from the molar fractions proposed by Escalante et al. (2012)

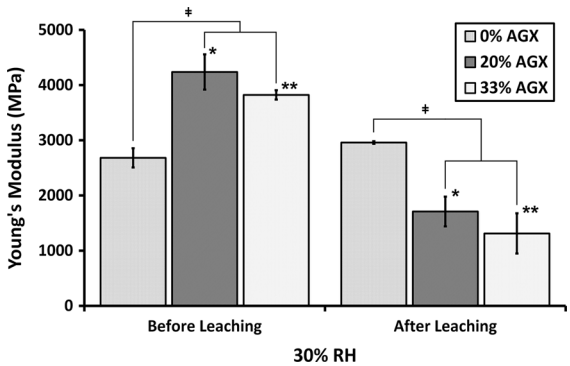

Fig. 8 Young's modulus of the regenerated cellulose (0 % AGX) and cellulose/AGX blend films (20 % AGX and 33 % AGX) at 30 % RH before and after leaching of the AGX. Each bar represents three replicates ± the standard deviation. (*Alveolar click*) Significant statistical difference of ($p \leq 0.05$) between 0 % AGX and 20 % AGX, 33 % AGX. No significant difference between 20 % AGX and 33 % AGX. (*Single asterisk*) Significant statistical difference of ($p \leq 0.05$) between 20 % AGX before leaching and 20 % AGX after leaching. (*Double asterisks*) Significant statistical difference of ($p \leq 0.05$) between 33 % AGX before leaching and 33 % AGX after leaching. No significant difference between 0 % AGX before leaching and 0 % AGX after leaching

in a weakening of the films indicating that the structure of the films was disrupted upon AGX removal. The regeneration kinetics and the resulting interactions between cellulose and AGX warrant further analysis to elucidate the governing mechanisms.

Conclusions

Cellulose and arabinoglucuronoxylan, isolated from the same tree were dissolved in EmimAc and regenerated with ethanol into clear optically transparent thin films with a smooth surface. SEM analysis of the cross section revealed internal porosity on a micro to nano scale. XRD showed that the films were amorphous after regeneration and that the composition did not affect the crystallinity. With some variation in the absolute values, the plasticizing effect of moisture on the films' tensile properties seems to be independent of film composition. The Young's modulus, maximum stress, and storage modulus all decreased with increasing humidity while the strain at break increased. The plasticizing effect of water on the films was also evidenced by DMA measurements. The similarities of the films with different composition in the tensile and DMA testing, together with the micro morphology similarities, indicate a regeneration process were the cellulose forms a network independently of the AGX content. The equilibrium moisture content at different relative humidities was clearly related to the mechanical properties. Stiffness of the blended films was higher than the pure cellulose film at 30 % RH. The strengthening effect was likely caused by cellulose/AGX interactions. We found good mechanical properties independent of the polysaccharide composition. Regeneration of cellulose/AGX blends from ionic liquids provides a novel route for production of films with tailored mechanical properties and shows potential of utilization of today unused renewable resources.

Acknowledgments The Knut and Alice Wallenberg Foundation is gratefully acknowledged for funding the Wallenberg Wood Science Center. Volodymyr Kuzmenko and Vratislav Langer are acknowledged for their assistance with the XRD analysis.

Conflict of interest The authors declare that there are no conflicts of interest.

References

Albersheim P, Darvill A, Roberts K, Sederoff R, Staehelin A (2010) Principles of cell wall architecture and assembly. Plant cell walls: from chemistry to biology. Garland Science, Taylor and Francis Group, London, pp 227–272

Bosmans TJ, Stépán AM, Toriz G, Renneckar S, Karabulut E, Wågberg L, Gatenholm P (2014) Assembly of debranched xylan from solution and on nanocellulosic surfaces. Biomacromolecules 15:924–930. doi:10.1021/bm4017868

Cao Y, Li H, Zhang Y, Zhang J, He J (2010) Structure and properties of novel regenerated cellulose films prepared from cornhusk cellulose in room temperature ionic liquids. J Appl Polym Sci 116:547–554

Dammström S, Gatenholm P (2008) Preparation and properties of cellulose/xylan nanocomposites. In: Characterization of the cellulosic cell wall. Blackwell, Oxford, pp 53–63. doi:10.1002/9780470999714.ch5

El Seoud OA, Koschella A, Fidale LC, Dorn S, Heinze T (2007) Applications of ionic liquids in carbohydrate chemistry: a window of opportunities. Biomacromolecules 8:2629–2647

Escalante A, Gonçalves A, Bodin A, Stepan A, Sandström C, Toriz G, Gatenholm P (2012) Flexible oxygen barrier films from spruce xylan. Carbohydr Polym 87:2381–2387

Fengel D, Wegener G (1983) Wood: chemistry, ultrastructure, reactions. Walter de Gruyter, Berlin

Fink HP, Weigel P, Purz HJ, Ganster J (2001) Structure formation of regenerated cellulose materials from NMMO-solutions. Prog Polym Sci 26:1473–1524. doi:10.1016/S0079-6700(01)00025-9

Froix MF, Nelson R (1975) The interaction of water with cellulose from nuclear magnetic resonance relaxation times. Macromolecules 8:726–730

Froschauer C, Hummel M, Iakovlev M, Roselli A, Schottenberger H, Sixta H (2013) Separation of hemicellulose and cellulose from wood pulp by means of ionic liquid/cosolvent systems. Biomacromolecules 14:1741–1750. doi:10.1021/bm400106h

Gröndahl M, Eriksson L, Gatenholm P (2004) Material properties of plasticized hardwood xylans for potential application as oxygen barrier films. Biomacromolecules 5:1528–1535

Hauru LKJ, Hummel M, King AWT, Kilpeläinen I, Sixta H (2012) Role of solvent parameters in the regeneration of cellulose from ionic liquid solutions. Biomacromolecules 13:2896–2905. doi:10.1021/bm300912y

Heredia A, Jiménez A, Guillén R (1995) Composition of plant cell walls Zeitschrift für Lebensmittel. Untersuchung und Forschung 200:24–31

Höije A, Sternemalm E, Heikkinen S, Tenkanen M, Gatenholm P (2008) Material properties of films from enzymatically tailored arabinoxylans. Biomacromolecules 9:2042–2047. doi:10.1021/bm800290m

Howsmon JA (1949) Water sorption and the poly-phase structure of cellulose fibers. Text Res J 19:152–162

Isobe N, Kim U-J, Kimura S, Wada M, Kuga S (2011) Internal surface polarity of regenerated cellulose gel depends on the species used as coagulant. J Colloid Interface Sci 359:194–201

Kilpeläinen I, Xie H, King A, Granstrom M, Heikkinen S, Argyropoulos DS (2007) Dissolution of wood in ionic liquids. J Agric Food Chem 55:9142–9148

Klemm D, Heublein B, Fink H-P, Bohn A (2005) Cellulose: fascinating biopolymer and sustainable raw material. Angew Chem Int Ed 44:3358–3393. doi:10.1002/anie.200460587

Köhnke T, Pujolras C, Roubroeks JP, Gatenholm P (2008) The effect of barley husk arabinoxylan adsorption on the properties of cellulose fibres. Cellulose 15:537–546

Kosan B, Michels C, Meister F (2008) Dissolution and forming of cellulose with ionic liquids. Cellulose 15:59–66

Laity P, Glover P, Hay J (2002) Composition and phase changes observed by magnetic resonance imaging during non-solvent induced coagulation of cellulose. Polymer 43:5827–5837

Lerouxel O, Cavalier DM, Liepman AH, Keegstra K (2006) Biosynthesis of plant cell wall polysaccharides—a complex process. Curr Opin Plant Biol 9:621–630

Lindman B, Karlström G, Stigsson L (2010) On the mechanism of dissolution of cellulose. J Mol Liq 156:76–81

Mäki-Arvela P, Anugwom I, Virtanen P, Sjöholm R, Mikkola J-P (2010) Dissolution of lignocellulosic materials and its constituents using ionic liquids—a review. Ind Crops Prod 32:175–201

Medronho B, Lindman B (2014) Competing forces during cellulose dissolution: from solvents to mechanisms. Curr Opin Colloid Interface Sci 19:32–40

Medronho B, Romano A, Miguel MG, Stigsson L, Lindman B (2012) Rationalizing cellulose (in) solubility: reviewing basic physicochemical aspects and role of hydrophobic interactions. Cellulose 19:581–587

Nakamura K, Hatakeyama T, Hatakeyama H (1981) Studies on bound water of cellulose by differential scanning calorimetry. Text Res J 51:607–613. doi:10.1177/004051758105100909

Nakamura K, Hatakeyama T, Hatakeyama H (1983) Effect of bound water on tensile properties of native cellulose. Text Res J 53:682–688. doi:10.1177/004051758305301108

Östlund Å, Idström A, Olsson C, Larsson PT, Nordstierna L (2013) Modification of crystallinity and pore size distribution in coagulated cellulose films. Cellulose 20:1657–1667

Pinkert A, Marsh KN, Pang S, Staiger MP (2009) Ionic liquids and their interaction with cellulose. Chem Rev 109:6712–6728. doi:10.1021/cr9001947

Ragauskas AJ et al (2006) The path forward for biofuels and biomaterials. Science 311:484–489. doi:10.1126/science.1114736

Reiter W-D (2002) Biosynthesis and properties of the plant cell wall. Curr Opin Plant Biol 5:536–542

Rogers RD, Seddon KR (2003) Ionic liquids-solvents of the future? Science 302:792–793. doi:10.1126/science.1090313

Salmen N, Back G (1977) The influence of water on the glass transition temperature of cellulose. Tappi 60:137–140

Šimkovic I, Tracz A, Kelnar I, Uhliariková I, Mendichi R (2014) Quaternized and sulfated xylan derivative films. Carbohydr Polym 99:356–364

Simmons TJ et al (2011) Preparation of synthetic wood composites using ionic liquids. Wood Sci Technol 45:719–733

Sun Q, Mandalika A, Elder T, Nair SS, Meng X, Huang F, Ragauskas AJ (2014) Nanocomposite film prepared by depositing xylan on cellulose nanowhiskers matrix. Green Chem 16:3458–3462

Sundberg J, Toriz G, Gatenholm P (2013) Moisture induced plasticity of amorphous cellulose films from ionic liquid. Polymer 54:6555–6560

Swatloski RP, Spear SK, Holbrey JD, Rogers RD (2002) Dissolution of cellose with ionic liquids. J Am Chem Soc 124:4974–4975

Theander O, Westerlund EA (1986) Studies on dietary fiber. 3. Improved procedures for analysis of dietary fiber. J Agric Food Chem 34:330–336. doi:10.1021/jf00068a045

Timell T (1961) Isolation of galactoglucomannans from the wood of gymnosperms. Tappi 44:88–96

Torimoto T, Tsuda T, Okazaki K, Kuwabata S (2009) New frontiers in materials science opened by ionic liquids. Adv Mater Weinheim 22:1196–1221

Troshenkowa S, Wawro D (2010) Dissolved state of cellulose in ionic liquids—the impact of water. Fibres Text East Eur 18:80

Turner MB, Spear SK, Holbrey JD, Rogers RD (2004) Production of bioactive cellulose films reconstituted from ionic liquids. Biomacromolecules 5:1379–1384

Wise LE, Murphy M, D'Addieco AA (1946) Chlorite holocellulose, its fractionation and bearing on summative wood analysis and on studies on the hemicelluloses. Pap Trade J 122:35–42

Wu RL, Wang XL, Li F, Li HZ, Wang YZ (2009) Green composite films prepared from cellulose, starch and lignin in room-temperature ionic liquid. Bioresour Technol 100:2569–2574

Zhang H, Wu J, Zhang J, He J (2005) 1-Allyl-3-methylimidazolium chloride room temperature ionic liquid: a new and powerful nonderivatizing solvent for cellulose. Macromolecules 38:8272–8277

Zhao Q, Yam RCM, Zhang B, Yang Y, Cheng X, Li RKY (2009) Novel all-cellulose ecocomposites prepared in ionic liquids. Cellulose 16:217–226

Zhu S et al (2006) Dissolution of cellulose with ionic liquids and its application: a mini-review. Green Chem 8:325–327

Zografi G, Kontny M, Yang A, Brenner G (1984) Surface area and water vapor sorption of macrocrystalline cellulose. Int J Pharm 18:99–116